Inorg. Chem. **2005**, *44*, 6174–6182

Theoretical Study on the Spin-State Energy Splittings and Local Spin in Cationic [Re]–C_n–[Re] Complexes

Carmen Herrmann,[†] Johannes Neugebauer,[‡] John A. Gladysz,[§] and Markus Reiher*[,†]

Institut für Physikalische Chemie, Friedrich-Schiller-Universität Jena, Helmholtzweg 4, D-07743 Jena, Germany, Afd. Theoretische Chemie, Vrije Universiteit Amsterdam, De Boelelaan 1083, 1081 HV Amsterdam, The Netherlands, and Institut für Organische Chemie, Universität Erlangen-Nürnberg, Henkestrasse 42, D-91054 Erlangen, Germany

Received February 15, 2005

Total spin-state energy splittings are calculated for mono- and dications of the formula $\{[Re]–C_n–[Re]\}^{z+}$ where [Re] = η^5-(C_5Me_5)Re(NO)(PPh_3). C_n is an even-numbered carbon chain with n ranging from 4 to 20, and z is 1 or 2. These complexes are experimentally known, and their potential role as molecular electronic devices initiated this work. We have considered the different total spin states monocation/doublet, monocation/quartet, dication/singlet, and dication/triplet. Data obtained for two density functionals BP86 and B3LYP* were compared to verify the internal consistency of the results. In both ionization states, the low-spin state is the ground state, but the spin-state splittings decrease as the chain gets longer. For the dications, the splitting reaches a nearly constant value of about 10 kJ/mol with BP86 and about 4 kJ/mol with B3LYP* when there are at least 14 carbon atoms in the chain, whereas for the monocations, no constant value appears to be reached asymptotically, not even if 20 carbon atoms are in the chain. For monocations, the splittings range from 138 kJ/mol ($n = 4$) to 68 kJ/mol ($n = 20$) with BP86 and from 134 kJ/mol ($n = 4$) to 73 kJ/mol ($n = 20$) with B3LYP* and are thus considerably higher than those of the dications. The spin-state splittings are qualitatively mirrored by the energy splitting between the highest-occupied molecular orbital with β spin ($HOMO_\beta$) and the lowest-unoccupied molecular orbital with α spin ($LUMO_\alpha$) as obtained in the low-spin state. Furthermore, the $HOMO_\alpha$–$LUMO_\alpha$ gaps decrease as the carbon chain lengthens. In addition, the local distribution of the $\hat{S}_z$ expectation value is analyzed for the monocation/doublet, the monocation/quartet, and the dication/triplet state using a modified Löwdin partitioning scheme. In the monocation/doublet and the dication/triplet state, the electron spin is distributed mainly on the metal centers and slightly delocalized onto the carbon chain. In the monocation/quartet state for chain lengths of more than 8 carbon atoms, the electron spin is mainly localized on selected atoms of the chain and not on the metal centers. In all cases, the spin delocalization onto the chain increases as the chain gets longer.

1. Introduction

Molecules with a one-dimensional unsaturated structure are currently under intense investigation to assess their potential role as molecular wires.[1−5] Molecular wires can, in principle, serve as building units in molecular scale electronic materials and nanotechnological devices such as electrical conductors,[6] light-emitting diodes,[7] and photovoltaic cells.[8] The synthesis and experimental characterization of such systems is an active and challenging area of current

* To whom correspondence should be addressed. E-mail: markus.reiher@uni-jena.de.
[†] Friedrich-Schiller-Universität Jena.
[‡] Vrije Universiteit Amsterdam.
[§] Universität Erlangen-Nürnberg.

(1) Metzger, R. M. *Chem. Rev.* **2003**, *103*, 3803−3834.
(2) Robertson, N.; McGowan, C. A. *Chem. Soc. Rev.* **2003**, *32*, 96−103.
(3) Aviram, A.; Ratner, M. A. *Molecular Electronics: Science and Technology;* New York Academy of Sciences: New York, 1998.
(4) Datta, S. *Electronic Transport in Mesoscopic Systems;* Cambridge University Press: Cambridge, U.K., 1995.
(5) Jortner, J.; Ratner, M. *Molecular Electronics;* Blackwell Science: Oxford, U.K., 1997.
(6) Nakashini, H.; Sumi, N.; Ueno, S.; Takiyima, K.; Aso, Y.; Otsubo, T.; Komaguchi, K.; Shiotani, M.; Ohta, N. *Synth. Met.* **2001**, *119*, 413.
(7) Kraft, A.; Grimsdale, A. C.; Holmes, A. B. *Angew. Chem., Int. Ed.* **1998**, *37*, 403−428.
(8) Harrison, M. G.; Friend, R. H. In *Electronic Materials: The Oligomer Approach;* Müllen, K., Wegner, G., Eds.; Wiley-VCH: Weinheim, Germany, 1998.

10.1021/ic050240l CCC: $30.25
Published on Web 08/11/2005

research (for a review, see ref 9). Because of the recent advances in these fields, an efficient tuning of the properties of molecular wires is becoming possible. In particular, the dependence of charge transport through molecular wires on their steric and electronic structure is an issue being investigated by various experimental groups.[10−12] On the basis of that work, molecular wires with optimal charge transport properties are being synthesized.[13−16]

One way of manipulating charge transport properties is to control the total spin state of the system, which can be achieved by applying a magnetic field. From research in the field of spintronics, it is known that in magnetic semiconductor devices many parameters, such as diffusion lengths or potential barriers, are spin dependent.[17] Also on a molecular scale, electron transport properties have been reported to depend on molecular spin states.[18] From a theoretical point of view, changes in the total spin will affect the energetics of the molecular orbitals as well as the local spin distribution of the system. Relating these changes in auxiliary quantities to observable properties in a systematic fashion is likely to finally help increase the understanding and control of charge transport through molecular wires.

Because the electronic structure of one-dimensional unsaturated structures attached to electrodes or metal fragments is, in general, complicated, it is not always possible to rely on well-established rules of thumb to predict structure−property relationships. Thus, quantum chemical calculations on the electronic structure are an essential tool for understanding and predicting the properties of molecular wires. They can help to guide experimental research toward the systems which are most appealing because of their steric and electronic structures and which are thus worth the effort of elaborate experimental work. Moreover, the calculations allow us to access features of the electronic structure which are not accessible experimentally. Theoretical investigations of the electronic structure of molecular wires include, e.g., calculations of the local charge distribution, HOMO−LUMO gaps, and vibrational frequencies.[19−21,30]

In this work, we focus on one-dimensional sp carbon chains clamped by two metal fragments. This topic has recently been reviewed (see refs 22−25), and many such complexes have been isolated by one of the present authors (see, e.g., refs 15 and 16). Complexes of this type have also been described by Lapinte, and some of these have been computationally investigated for short chain lengths.[30] For other complexes that can be isolated in more than one redox state, see refs 19 and 31.

Of special interest is the dependence of molecular properties, such as conformational stability, charge distribution, and vibrational states, on the length of the carbon chain. We will concentrate here on properties which are related to electron spin, in particular total spin-state energy splittings and the local electron-spin distribution within the molecules. As mentioned above, these electron-spin properties of sp carbon wires can have a considerable influence on their charge-transfer properties. We investigate two oxidized forms of a [Re]−C_n−[Re] complex (with n being an even number), the monocation and the dication, in two different total spin states each, the doublet and quartet states for the monocation and the singlet and triplet states for the dication. In contrast to other theoretical investigations of long sp carbon chains with metal endgroups reported so far,[21] we have analyzed these molecules with their full set of ligands and extend our previous study on neutral chain-linked rhenium complexes, which was devoted to the vibrations of the carbon chain.[32] Furthermore, we have supplemented our calculations with the pure density functional BP86 by a comparison with the B3LYP* hybrid functional, which is known to give a better description of total spin splittings than standard functionals[33−35] (see also the excellent comparative account by Harvey[36]), to probe the reliability of the DFT results.

This paper is organized as follows: In section 2, a brief overview of the computational methods employed in this work and the theory of local $\langle \hat{S}_z \rangle$ values is given. The effects of changes in the total spin state and charge on the molecular geometry are briefly summarized in section 3. In section 4, spin-state splittings from total energy expectation values are reported for carbon chain lengths ranging from 4 to 20 carbon

(9) Martin, R. E.; Diederich, F. *Angew. Chem., Int. Ed.* **1999**, *38*, 1350−1377.
(10) Giacaleone, F.; Segura, J. L.; Martin, N.; Guldi, D. M. *J. Am. Chem. Soc.* **2004**, *126*, 5340.
(11) Vail, S. A.; Tome, J. P. C.; Krawczuk, P. J.; Dourandin, A.; Shafirovich, V.; Cavaleiro, J. A. S.; Schuster, D. I. *J. Phys. Org. Chem.* **2004**, *17*, 814.
(12) Weiss, E. A.; Ahrens, M. J.; Sinks, L. E.; Ratner, M. A.; Wasielewski, M. R. *J. Am. Chem. Soc.* **2004**, *126*, 5577.
(13) Imahori, H.; Guldi, D. M.; Tamaki, K.; Yoshida, Y.; Luo, C.; Sakata, Y.; Fukuzumi, S. *J. Am. Chem. Soc.* **2001**, *123*, 6617−6628.
(14) Fukuzumi, S.; Imahori, H. *Mol. Supramol. Photochem.* **2003**, 227.
(15) Dembinski, R.; Bartik, T.; Bartik, B.; Jaeger, M.; Gladysz, J. A. *J. Am. Chem. Soc.* **2000**, *122*, 810−822.
(16) Mohr, W.; Stahl, J.; Hampel, F.; Gladysz, J. A. *Chem.−Eur. J.* **2003**, *9*, 3324−3340.
(17) Lebedeva, N.; Kuivalainen, P. *J. Appl. Phys.* **2003**, *93*, 9845−9864.
(18) Park, J.; Pasupathy, A. N.; Goldsmith, J. I.; Chang, C.; Yaish, Y.; Petta, J. R.; Rinkoski, M.; Sethna, J. P.; Abruna, H. D.; McEuen, P. L.; Ralph, D. C. *Nature* **2002**, *147*, 722−725.
(19) Bruce, M. I.; Low, P. J.; Costuas, K.; Halet, J.-F.; Best, S. B.; Heath, G. A. *J. Am. Chem. Soc.* **2000**, *122*, 1949−1962.
(20) Bruce, M. I.; Halet, J.-F.; Le Guennic, B.; Skelton, B. W.; Smith, M. E.; White, A. H. *Inorg. Chim. Acta* **2003**, *350*, 175−181.
(21) Zhuralev, F.; Gladysz, J. A. *Chem.−Eur. J.* **2004**, *10*, 6510−6522.
(22) Bruce, M. I.; Low, P. J. *Adv. Organomet. Chem.* **2004**, *50*, 179−444.
(23) Szafert, S.; Gladysz, J. A. *Chem. Rev.* **2003**, *103*, 4175−4206.
(24) Paul, F.; Lapinte, C. *Coord. Chem. Rev.* **1998**, *178−180*, 431.
(25) Paul, F.; Lapinte, C. Magnetic Communication in Binuclear Organometallic Complexes Mediated by Carbon-Rich Bridges. In *Unusual Structures and Physical Properties in Organometallic Chemistry*; Gielen, M., Willem, R., Wrackmyer, B., Eds.; Wiley: New York, 2002.
(26) Narvor, N. L.; Toupet, L.; Lapinte, C. *J. Am. Chem. Soc.* **1995**, *117*, 7129.
(27) Guillemot, M.; Toupet, L.; Lapinte, C. *Organometallics* **1998**, *17*, 1928.
(28) Narvor, N. L.; Lapinte, C. *C. R. Acad. Sci.* **1998**, *1*, 745−807.
(29) Paul, F.; Meyer, W. E.; Toupet, L.; Jiao, H.; Gladysz, J. A.; Lapinte, C. *J. Am. Chem. Soc.* **2000**, *122*, 9405−9414.
(30) Jiao, H.; Costuas, K.; Gladysz, J. A.; Halet, J.-F.; Guillemot, M.; Toupet, L.; Paul, F.; Lapinte, C. *J. Am. Chem. Soc.* **2003**, *125*, 9511−9522.
(31) Kheradmandan, S.; Heinze, K.; Schmalle, H. W.; Berke, H. *Angew. Chem., Int. Ed.* **1999**, *38*, 2270−2273.
(32) Neugebauer, J.; Reiher, M. *J. Phys. Chem. A* **2004**, *108*, 2053−2061.
(33) Reiher, M.; Salomon, O.; Hess, B. A. *Theor. Chem. Acc.* **2001**, *107*, 48−55.
(34) Reiher, M. *Inorg. Chem.* **2002**, *41*, 6928−6935.
(35) Salomon, O.; Reiher, M.; Hess, B. A. *J. Chem. Phys.* **2002**, *117*, 4729−4737.
(36) Harvey, J. N. *Struct Bonding* **2004**, *112*, 151−183.

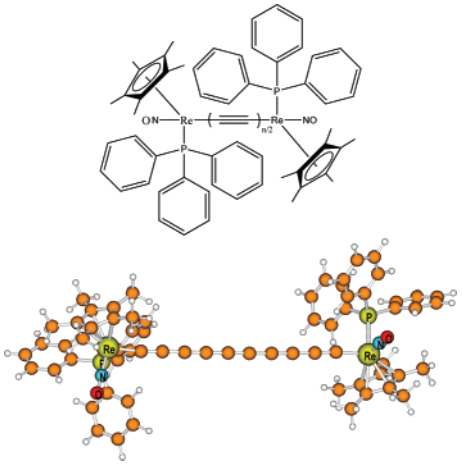

Figure 1. Lewis structure of the neutral compound [Re]−C_n−[Re] with [Re] = η^5-(C_5Me_5)Re(NO)(PPh_3) and optimized geometry for the doublet state of the monocation with $n = 10$ (BP86/RI, TZVP).

atoms for the mono- and dicationic complexes. After the discussion of the theoretical background for our interpretation of molecular orbital energies in section 5.1, these splittings are compared to the orbital energy splittings $HOMO_\alpha$−$LUMO_\beta$ and $HOMO_\beta$−$LUMO_\alpha$, respectively, in section 5.2. Furthermore, in section 5.3, the $HOMO_\alpha$−$LUMO_\alpha$ gap is investigated. In section 6, the local $\langle \hat{S}_z \rangle$ distribution for the monocation/doublet, the monocation/quartet, and the dication/triplet is analyzed. Our results are summarized in section 7.

2. Quantum Chemical Methodology

Density functional theory (DFT) calculations were carried out for mono- and dications of [Re]−C_n−[Re] where [Re] = η^5-(C_5Me_5)Re(NO)(PPh_3) and the number of carbon atoms in the chain, *n*, is an even number between 4 and 20 (Figure 1) (low-spin states of the neutral species are also available from our previous work[32]). Note that we have *not* simplified the ligand structure by replacing Cp* by Cp or PPh_3 by PH_3. For each chain length, there are four different electronic structures to be calculated: a monocation/doublet, a monocation/quartet, a dication/singlet, and a dication/triplet state. To ensure that all relevant spin states have been taken into consideration, we calculated the next-highest spin states (the monocation/sextet and dication/quintet for the compound with $n = 4$ as test case), which turned out to be significantly higher in energy than the two total spin states reported in this paper for both cations.

All structures were fully optimized with BP86[37,38] (in combination with the resolution-of-the-identity (RI) density-fitting technique[39−41]). To test the dependence of the results on the density functional chosen, we applied our B3LYP* functional,[33−35] which is well suited for the calculation of the spin-state splittings. Since the B3LYP* calculations are time-consuming, we selected only every second structure (i.e., we elongated the chain by four carbon atoms starting at [Re]−C_4−[Re], followed by [Re]−C_8−[Re], etc.) and carried out single-point calculations on the BP86/RI-optimized structures. We have used Ahlrichs' TZVP basis set[42] throughout, which features a valence triple-ζ basis set with polarization functions on all atoms. For the rhenium atoms, the effective large-core potentials of the Stuttgart group were employed (which also account for the scalar relativistic effects).[43] These potentials include 60 electrons of the inner shells (i.e., the 15 electrons belonging to the 5s, 5p, 5d, and 6s shells are treated explicitly). All calculations were performed with the TURBOMOLE program package.[44] Molecular structures and orbitals were visualized with the program MOLDEN.[45] For the calculation of local contributions to the total $\langle \hat{S}_z \rangle$ value, we applied our implementation[46] of local spin analyses by $\hat{S}^2$- and $\hat{S}_z$-partitioning in TURBOMOLE which relies on the theoretical work on local spin by Clark and Davidson.[47−49]

To avoid confusion between local portions of $\langle \hat{S}_z \rangle$ and quantities such as "atomic spin densities", a very brief review of the essential theory of $\hat{S}_z$-partitioning is given in the following. The total $\langle \hat{S}_z \rangle$ expectation value is equal to the total spin quantum number M_S. For a single Slater determinant with little spin contamination (i.e. $M_S \approx S$), the $\langle \hat{S}_z \rangle$ value yields indirectly the total molecular electron spin *S*. The idea is now to decompose the total $\langle \hat{S}_z \rangle$ expectation value of such non-spin-contaminated Slater determinants into atomic contributions, which give information on how much electron spin is located on that atom. The total $\hat{S}_z$ operator shall thus be written as a sum of local operators $\hat{S}_{zA}$

$$\hat{S}_z = \sum_A \hat{S}_{zA} \tag{1}$$

The sum is running over any set of local subsystems (atoms) A of the molecule which add correctly to the total system. To construct such local operators as $\hat{S}_{zA}$, Clark and Davidson[47] have introduced a projection operator technique, where hermitean one-electron projectors onto the subsystems, $\hat{p}_A$, are employed. Provided these projectors total one when the sum is running over the whole set of subsystems

$$\sum_A \hat{p}_A(i) = \hat{1}(i) \tag{2}$$

they can be inserted into the one-electron operator decomposition of $\hat{S}_z$

$$\hat{S}_z = \sum_i^N \hat{s}_z(i) = \sum_i^N \hat{s}_z(i)\hat{1}(i) = \sum_i^N \hat{s}_z(i) \sum_A \hat{p}_A(i) = \sum_A \sum_i^N \hat{s}_z(i)\hat{p}_A(i) = \sum_A \hat{S}_{zA} \tag{3}$$

where the definition of the local $\hat{S}_{zA}$ operator

(37) Becke, A. D. *Phys. Rev. A* **1988**, *38*, 3098−3100.
(38) Perdew, J. P. *Phys. Rev. B* **1986**, *33*, 8822−8824.
(39) Dunlap, B. I.; Connolly, J. W. D.; Sabin, J. R. *J. Chem. Phys.* **1979**, *71*, 3396−3402.
(40) Eichkorn, K.; Treutler, O.; Öhm, H.; Häser, M.; Ahlrichs, R. *Chem. Phys. Lett.* **1995**, *240*, 283−290.
(41) Eichkorn, K.; Weigend, F.; Treutler, O.; Ahlrichs, R. *Theor. Chem. Acc.* **1997**, *97*, 119−124.
(42) Schäfer, A.; Huber, C.; Ahlrichs, R. *J. Chem. Phys.* **1994**, *100*, 5829−5835.
(43) Andrae, D.; Häussermann, U.; Dolg, M.; Stoll, H.; Preuss, H. *Theor. Chim. Acta* **1990**, *77*, 123−141.
(44) Ahlrichs, R.; Bär, M.; Häser, M.; Horn, H.; Kölmel, C. *Chem. Phys. Lett.* **1989**, *162*, 165.
(45) Schaftenaar, G.; Noordik, J. H. *J. Comput.-Aided Mol. Des.* **2000**, *14*, 123−134.
(46) Herrmann, C.; Reiher, M.; Hess, B. A. *J. Chem. Phys.* **2005**, *122*, 034102.
(47) Clark, A. E.; Davidson, E. R. *J. Chem. Phys.* **2001**, *115*, 7382−7392.
(48) Davidson, E. R.; Clark, A. E. *Mol. Phys.* **2002**, *100*, 373−383.
(49) Clark, A. E.; Davidson, E. R. *J. Phys. Chem. A* **2002**, *106*, 6890−6896.

$$\hat{S}_{zA} = \sum_{i}^{N} \hat{s}_z(i)\hat{p}_A(i) \tag{4}$$

emerges naturally. Its expectation value for a single Slater determinant is half the difference between the number of α and β electrons on subsystem A, N^{α}_{A}, and N^{β}_{A}, respectively

$$\langle \hat{S}_{zA} \rangle = \frac{1}{2}(N^{\alpha}_{A} - N^{\beta}_{A}) \tag{5}$$

$N^{\alpha}_{A} - N^{\beta}_{A}$ is known as the "atomic spin density" in the literature, and the factor 1/2 stems from the spin properties of electrons as fermions. N^{α}_{A} could also be called the α-electron population of center A. Of course, as in any population analysis, N^{α}_{A} and N^{β}_{A} depend on the choice of the local projection operator, $\hat{p}_A$. The definition of this local projection operator poses a problem to which no unambiguous solution exists. There are a variety of atomic decomposition schemes reported in the literature, such as the Mulliken,[50] Löwdin,[51] PABOON,[52] and Bader's atoms-in-molecules approaches,[53] just to mention a few (for a review on population analyses, see refs 54 and 55 and for population analysis with projection operators, see ref 56). In this work, we have used modified Löwdin projectors for the decomposition of $\langle \hat{S}_z \rangle$ into atomic contributions, initially proposed by Clark and Davidson.[47] These modified projectors, denoted "Löwdin*" in the following, differ from the standard Löwdin projectors by an orthonormalization of the (atom-centered) basis functions within each atomic center prior to the conventional Löwdin orthonormalization. We found that these Löwdin* projectors yield local $\langle \hat{S}_z \rangle$ values very close to the corresponding atoms-in-molecules values,[46] which are very appealing from a formal point of view, but considerably more involved to calculate because they have to be evaluated numerically in contrast to the Löwdin scheme.

3. Dependence of the Molecular Geometry on the Total Charge and Spin State

Before investigating the effect of changes in the molecular total charge and spin state on the electronic structure, the effect of these changes on the molecular geometry of the mono- and dications $\{[Re]-C_n-[Re]\}^{z+}$ shall be summarized. Regardless of the chain length, the total spin state, and the total charge, the C−C bond lengths in the carbon chain do not vary much along the chain and range at most from 1.27 to 1.31 Å (see Supporting Information), which in comparison to the mean value of C−C single, double, and triple bonds (which are 1.54, 1.34, and 1.20 Å, respectively[68]) suggests that the electronic structure of the carbon chain is represented best by an allene-like sequence of double bonds in all cationic molecular structures under study here.

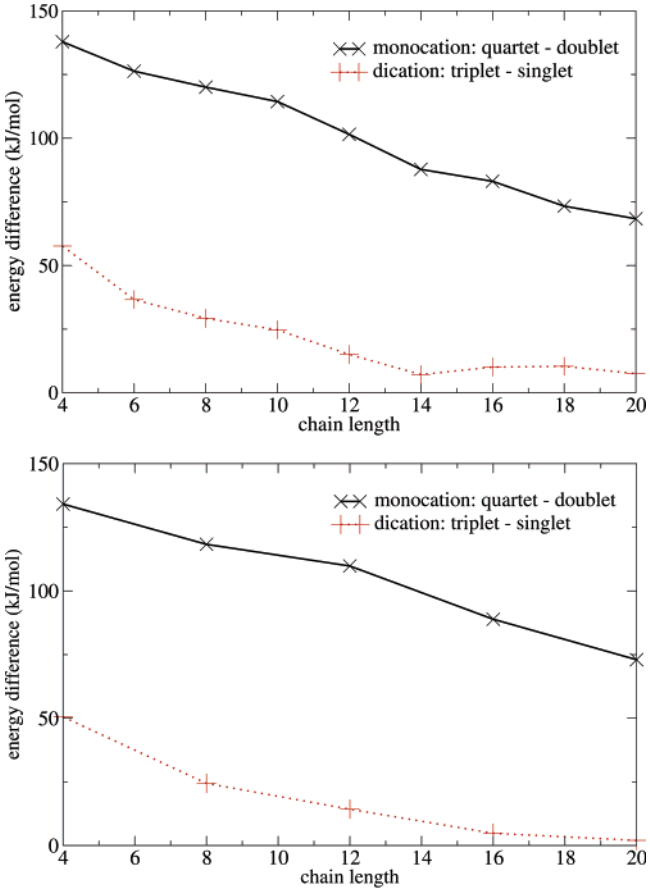

Figure 2. Total energy splitting of monocations (quartet−doublet) and dications (triplet−singlet) obtained with the pure density functional BP86/RI (top) and the modified hybrid functional B3LYP* (bottom). The low-spin state is always the ground state.

4. Spin-State Splittings from the Total Energy Expectation Values

First, the total energy splitting between the low-spin state and a high-spin state of the mono- and dication shall be investigated as a function of the carbon chain length. For the monocation, these are the doublet and the quartet state, and for the dication, the singlet and the triplet state. The structures for each charge and spin state are fully optimized with the BP86 functional and the TZVP basis set, using the RI approximation. The performances of the BP86 and the B3LYP* functional are compared.

As can be seen in Figure 2, the energy splittings depend only little on the functional chosen, and consistent results

(50) Mulliken, R. S. *J. Chem. Phys.* **1955**, *23*, 1833−1840.
(51) Löwdin, P.-O. *J. Chem. Phys.* **1950**, *18*, 365−375.
(52) Heinzmann, R.; Ahlrichs, R. *Theor. Chim. Acta* **1976**, *42*, 33−45.
(53) Bader, R. F. W. *Atoms in Molecules: A Quantum Theory;* Oxford University Press: New York, 1994.
(54) Meister, J.; Schwarz, W. H. E. *J. Phys. Chem.* **1994**, *98*, 8245−8252.
(55) Bachrach, S. M. In *Reviews in Computational Chemistry*, Vol. 5; Lipkowitz, K. B., Boyd, D. B., Eds.; VCH Publishers: New York, 1994; p 171−227.
(56) Clark, A. E.; Davidson, E. R. *Int. J. Quantum Chem.* **2003**, *93*, 384−394.
(57) Koopmans, T. *Physica* **1934**, *1*, 104−113.
(58) Foster, J. M.; Boys, S. F. *Rev. Mod. Phys.* **1960**, *32*, 296−299.
(59) Edmiston, C.; Ruedenberg, K. *J. Chem. Phys.* **1965**, *43*, S97−S116.
(60) Pipek, J.; Mezey, P. G. *J. Chem. Phys.* **1989**, *90*, 4916−4926.
(61) Magnasco, V.; Perico, A. *J. Chem. Phys.* **1972**, *47*, 971−981.
(62) Helgaker, T.; Jørgensen, P.; Olsen, J. *Molecular Electronic-Structure Theory;* Wiley VCH: New York, 2000.
(63) Gritsenko, O. V.; Braïda, B.; Baerends, E. J. *J. Chem. Phys.* **2003**, *119*, 1937−1950.
(64) Chong, D. P.; Gritsenko, O. V.; Baerends, E. J. *J. Chem. Phys.* **2002**, *116*, 1760−1772.
(65) Gritsenko, O. V.; Baerends, E. J. *J. Chem. Phys.* **2002**, *117*, 9154−9159.
(66) Gritsenko, O. V.; Baerends, E. J. *J. Chem. Phys.* **2004**, *120*, 8364−8372.
(67) Salzner, U.; Pickup, P. G.; Poirier, R. A.; Lagowski, J. B. *J. Phys. Chem. A* **1998**, *102*, 2572−2578.
(68) Aylward, G. H.; Findlay T. J. V. *SI Chemical Data;* Wiley VCH: New York, 2002.

may be obtained with the BP86 functional, which allows us to speed up the calculations because of the RI technique. Thus, the complexes under study represent standard transition metal complexes with respect to the classification given in ref 34. The dications show an almost constant value of the splitting (of about 10 kJ/mol or 2.4 kcal/mol with BP86/RI and about 4 kJ/mol or 1 kcal/mol with B3LYP*) once a chain length of 14 carbon atoms is reached. In contrast to this, we have not reached a constant splitting in the case of the monocations even after having 20 carbon atoms in the chain. After the second ionization of an electron, the energy gap between the low-spin and high-spin states is vanishingly small, while it is quite large in the case of the monocations. Inclusion of exact exchange (like in B3LYP*) would decrease the splitting further so that the high-spin states might become the ground states if the chain is sufficiently long, and indeed, B3LYP* shows a smaller gap though the low-spin state is still the ground state. These theoretical predictions correspond well with experimental data obtained for Lapinte's dication $[Cp^*(dppe)Fe-C_4-Fe(dppe)Cp^*][PF_6]_2$. As proven by a number of techniques (magnetic susceptibility measurements and Mössbauer spectroscopy), the singlet and triplet states are very close in energy for this system.[28]

5. Interpretation of Orbital Energy Splittings

5.1. Theoretical Background. The calculations of the energy differences in the previous section involve the optimization of the two total spin states, which is rather time-consuming. To circumvent this, the energy splittings between two total spin states shall be compared to the energy splittings between molecular orbitals optimized for only one spin state. We thus aim at a correlation of (nonobservable) one-electron quantities with (observable) all-electron quantities. In case there is a reliable correlation between both splittings, the expensive total spin state splittings could be estimated from orbital energy splittings. The theoretical framework for such a correlation relies on two assumptions: first, a naive independent-particle model is employed, and second, the orbital relaxation is neglected. The first assumption implies that the total energy can be calculated as a sum over all occupied MO energies (as in an extended-Hückel model, for example), and the second assumption implies that the orbital energies do not change when going from one total spin state to another one.

The interpretation of the diagonal elements of the Lagrange multipliers matrix as molecular orbital energies is based on Koopmans' theorem,[57] which states that the first ionization energy can be approximated as the negative orbital energy of the highest-occupied molecular orbital (HOMO) and the first electron affinity can be approximated as the negative orbital energy of the lowest-unoccupied molecular orbital (LUMO). Koopmans' theorem derived for any set of Hartree−Fock molecular orbitals (i.e., for the canonical set as well as for any set of orthonormal orbitals generated from these by a unitary transformation, like a localization,[58−61] for example) relates the ionization energy to the Fock matrix elements.[62] Then, the cationic state is represented by a CI-like expansion into a basis of all Slater determinants which

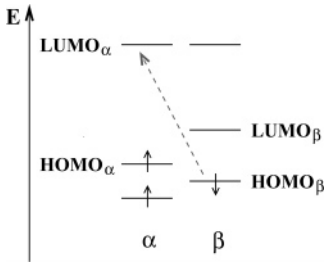

Figure 3. Qualitative molecular orbital energy diagram for the monocation/doublet state. The dotted arrow indicates the energy difference needed for the change to the quartet state within a naive independent-particle picture neglecting orbital relaxations. Although the picture suggests that the second doublet state is considerably lower in energy than the first quartet state, such a conclusion should not be drawn because the correlation between the HOMO−LUMO gaps and the excitation energies is not necessarily comparable for different procedures such as electronic excitations within a total spin state on one hand and changes between the total spin states on the other hand.

can be generated by removing one orbital from the Slater determinant minimizing the Hartree−Fock energy of the neutral state. The resulting energy difference between the two oxidation states is equal to a negative eigenvalue of a molecular orbital if the *canonical* Hartree−Fock orbitals are employed.[62] Therefore, an attempt to determine the energy differences of all-electron states from the orbital energies of chemically more intuitive localized orbitals is likely to be less reliable.

This is why we interpret *canonical* Kohn−Sham orbitals only. It has been shown by Baerends and co-workers that there exists an analogue for Koopmans' theorem for Kohn−Sham orbital energies,[63] which are interpreted as relaxed vertical ionization potentials.[64] This analogue is in particular applicable to open-shell systems which are described by spin-density functional theory.[65,66] Since our intention is furthermore to investigate from a pragmatic point of view whether Kohn−Sham orbital energies can be used for a qualitative prediction of total state energy differences, the correlation between the Kohn−Sham orbital energies and the total energy differences may be justified.

Within the unrestricted framework we are using here for all open-shell systems, all MOs are *spin* orbitals which consist of a spatial part multiplied by an α or β spin function. The classification of a MO as an α or β MO in this work denotes a spatial part of this MO to be multiplied with a α or β spin function, respectively. A transition from the low-spin to the high-spin state is described within this model by taking an electron out of the highest-occupied molecular orbital with β spin (HOMO$_\beta$) and occupying the lowest-unoccupied molecular orbital with α spin (LUMO$_\alpha$) as obtained in the low-spin state. A corresponding qualitative energy scheme which illustrates the transition from the doublet to the quartet state on the basis of the canonical Kohn−Sham orbitals optimized for the monocation/doublet state is given in Figure 3. The most relevant MOs are plotted in Figure 4. The orbital energies in Hartree are −0.251 (HOMO$_\alpha$ − 1), −0.223 (HOMO$_\alpha$), −0.166 (LUMO$_\alpha$), −0.249 (HOMO$_\beta$), −0.209 (LUMO$_\beta$), and −0.164 (LUMO$_\beta$ + 1) for a C_4 chain.

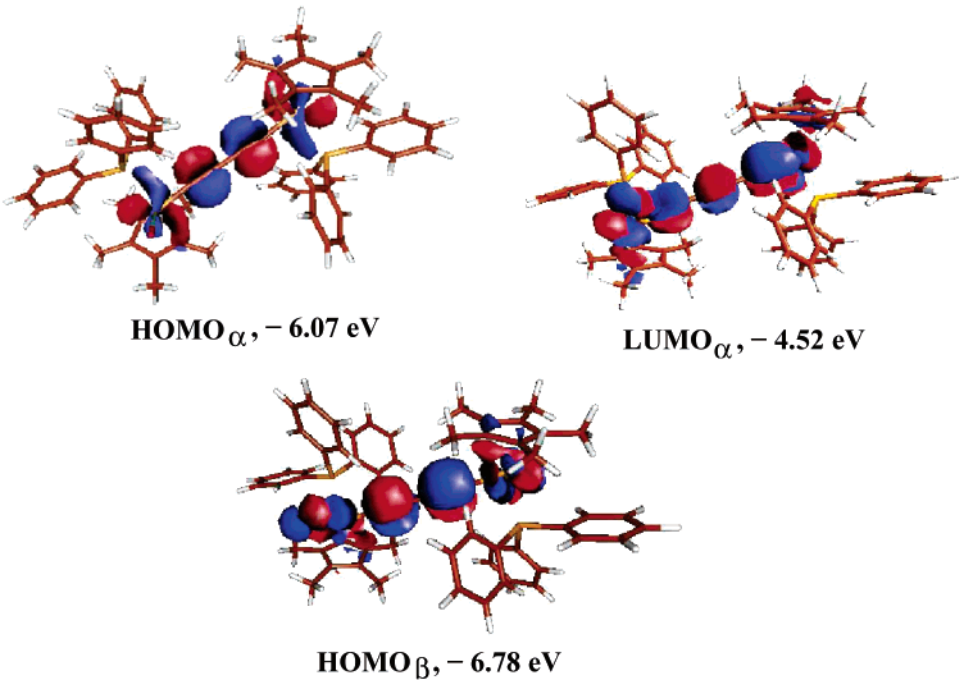

Figure 4. Selected molecular orbitals of the monocation of [Re]−C_4−[Re] in the doublet state (BP86/RI, TZVP).

Regarding this qualitative MO scheme, it can be seen that, neglecting orbital relaxation, the monocation/quartet state will differ from the monocation/doublet state only by the additional energy of an occupied (former) $LUMO_\alpha$, now $HOMO_\alpha$, and the missing energy of an unoccupied (former) $HOMO_\beta$, now $LUMO_\beta$. Thus, the energy difference between the two states is approximately given by the energy difference between $LUMO_\alpha$ and $HOMO_\beta$. The reverse consideration should also work, that is the total spin splitting might also be estimated from the $HOMO_\alpha$−$LUMO_\beta$ energy difference in the higher-spin state. We thus interpret HOMO−LUMO splittings in one spin state and extract information on a different electronic state (namely the other spin state) from a simple orbital inspection of the first spin state. As this is a rather crude qualitative picture (though often used in chemistry), it is interesting to see whether this assumption works. For this purpose, the energy splittings between $LUMO_\alpha$ and $HOMO_\beta$ for the lower-spin states (monocation/doublet and dication/singlet) and $HOMO_\alpha$ and $LUMO_\beta$ for the higher-spin states (monocation/quartet and dication/triplet) and their dependence on the chain length are investigated.

5.2. Orbital Energy Splittings $HOMO_\beta$−$LUMO_\alpha$ and $HOMO_\alpha$−$LUMO_\beta$. At first sight, the trends observed for the physically meaningful differences of total energy expectation values in section 4 are paralleled by the one-electron quantities (i.e., by the orbital energies) which are depicted as a function of the carbon chain length in Figure 5.

There are two curves which reproduce the qualitative behavior of the rigorously calculated spin-state energy splittings quite well. These are the $LUMO_\alpha$−$HOMO_\beta$ (monocation/doublet) and the $LUMO_\alpha$−$HOMO_\beta$ (dication/singlet) curve. On the other hand, the quantitative agreement of these curves with the true splittings is poor. The B3LYP*

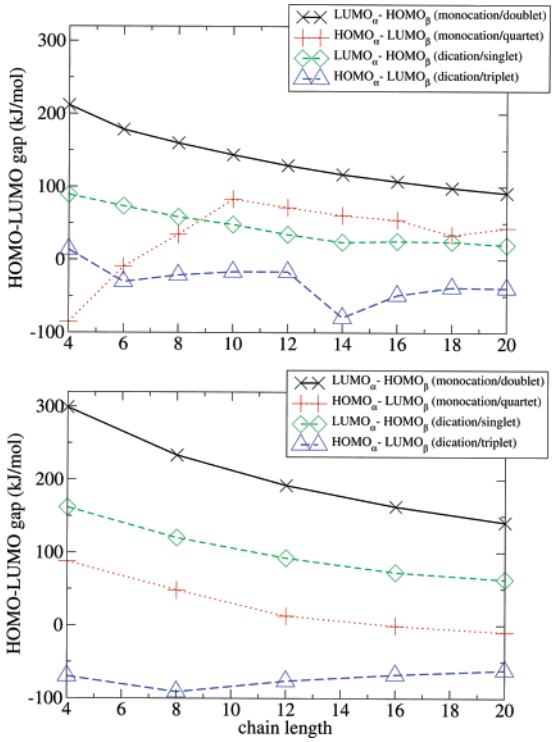

Figure 5. Gaps between the HOMO and LUMO α and β orbitals of monocations (quartet−doublet) and dications (triplet−singlet) obtained with the pure density functional BP86/RI (top) and the modified hybrid functional B3LYP* (bottom).

values even lead to an overestimation of the splitting energies by a factor of 2.

Furthermore, the two density functionals BP86 and B3LYP* do not give the same quantitative results. The orbital splittings are obviously much more affected by the choice of the density functional than the total spin state splittings. This is no surprise in view of the work by Salzner et al.[67]

and our own work,[33−35] which predict a significant dependence of splittings on the exact exchange admixture. We recall that for the total spin-state splittings, both functionals yielded quantitatively consistent values. Still, regarding the crude approximations made before, the qualitative agreement is remarkably good.

The two other curves $LUMO_\beta-HOMO_\alpha$ (monocation/quartet) and $LUMO_\beta-HOMO_\alpha$ (dication/triplet), which use the MOs optimized for the higher-spin states, do not give any valuable information on spin-state splittings. In some cases, they even predict an inverted energy relationship between the two total spin states (note the negative values on the *y* axis in Figure 5). Furthermore, the qualitative behavior of both curves changes considerably when using B3LYP* instead of BP86/RI. Altogether, this indicates the breakdown of the naive model for the estimate of spin-state splittings starting from the high-spin states. Thus, the $HOMO_\alpha-LUMO_\beta$ splittings obtained from the high-spin state should not be interpreted. But the important result is that we can indeed use the $HOMO_\beta-LUMO_\alpha$ splitting in the low-spin state to estimate the spin-state energy splitting.

5.3. Orbital Energy Splitting $HOMO_\alpha-LUMO_\alpha$. In the following section, the energy splittings between the HOMO (which is always the $HOMO_\alpha$) and the LUMO (to be more precise: the $LUMO_\alpha$) and their dependence on the chain length are investigated. Within the simple model described in the preceding section, these orbital energy splittings should allow predictions of the energy differences between the electronic ground state and the first electronically excited state within a given total spin state, without the effort of optimizing the excited states.

Since the absolute values depend strongly on the density functional, they can hardly be interpreted. Still, assuming that this approximate model is as reliable as in the preceding section as far as the *qualitative* behavior is concerned, it can be concluded from Figure 6 that the energy gap between the ground and first excited state decreases as the chain length increases for all of the charge/spin states. With respect to electron transport through the carbon chain, the decreasing HOMO−LUMO splitting implies that the conductivity increases with the chain length, as could be expected from considerations on the basis of qualitative MO theory. Furthermore, Figure 6 suggests that the first electronic excitation energies are similar for the monocation/doublet and the dication/triplet states. This similarity can be nicely explained by the simple independent-particle/neglect-of-orbital-relaxation model because both excitations employ the same set of two orbitals in this picture. Both functionals yield essentially the same qualitative behavior of the four curves, which supports the assumption that they display the qualitative features of the energy splittings correctly.

6. Local $\langle\hat{S}_z\rangle$ Distribution

To analyze where the excess spin is located (i.e., whether it resides on the bridge or on the metal centers), we have performed local $\langle\hat{S}_z\rangle$ analyses of the open-shell Slater determinants constructed with BP86/RI and B3LYP* orbitals for the dication/triplet, monocation/doublet, and monocation/quartet state. Since a local $\langle\hat{S}_z\rangle$ analysis of a closed-shell MO wave function necessarily yields zero for all atoms, we did not investigate the dication/singlet state.[46]

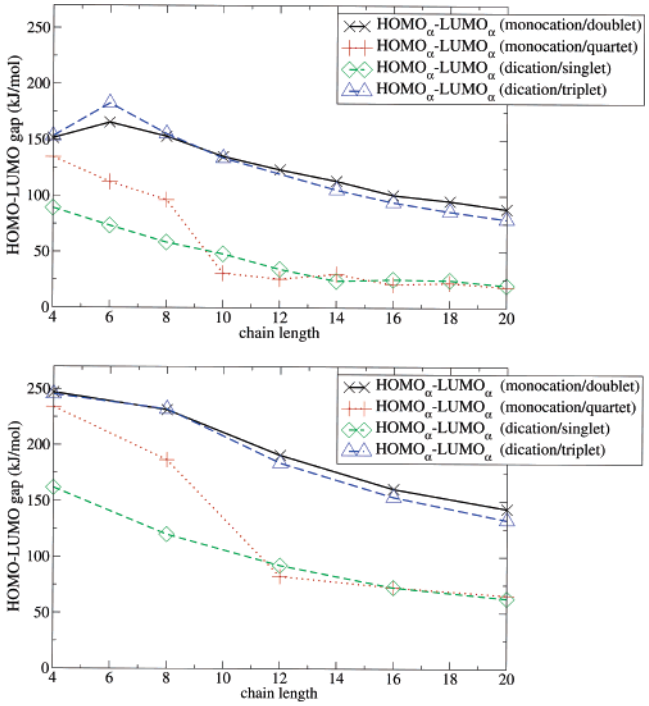

Figure 6. HOMO−LUMO gaps for α orbitals of monocations (quartet−doublet) and dications (triplet−singlet) obtained with the pure density functional BP86/RI (top) and the modified hybrid functional B3LYP* (bottom). Of course, since the α and *β* MOs in the dication/singlet state are identical, the $HOMO_\alpha-LUMO_\alpha$ (monocation/singlet) curves here are identical to the $LUMO_\alpha-HOMO_\beta$ (monocation/singlet) curves in Figure 5.

As mentioned above, the local $\langle\hat{S}_z\rangle$ values are related to what is known as the local (or atomic) spin densities by a factor of 1/2, a local $\langle\hat{S}_z\rangle$ value of 0.25 corresponds to a local spin density of 0.50. If the electron spin were completely located on the metal atoms and distributed symmetrically, one would expect local $\langle\hat{S}_z\rangle$ values of 0.5, 0.25, and 0.75 for the dication/triplet, monocation/doublet, and monocation/quartet states, respectively. In the case of the dication/triplet and monocation/doublet states, the local $\langle\hat{S}_z\rangle$ values on both of the rhenium atoms are indeed identical.

However, as can be seen in Figure 7, they are considerably smaller than 0.25 and 0.5, which is the result of a spin delocalization mainly onto the carbon chain atoms. The local spin on the chain atoms is always well below the local spin on the metal atoms, but as the chain length increases, this difference becomes smaller, and furthermore, the local spin on both the metal atom and the carbon chain atoms decrease. However, since all carbon chain atoms have approximately the same portion of local electron spin, the spin polarization decreases as the chain lengthens.

As far as the monocation/quartet state is concerned, the spin distribution is completely different. For a chain length from 10 to 20 carbon atoms, in all cases a pattern like Re-(•)C(○)C(•)C(○)C(•)C(○)... can be observed symmetrically on each side, where (•) means a small (typically around 0.05 atomic units) and (○) means a high (typically around 0.15

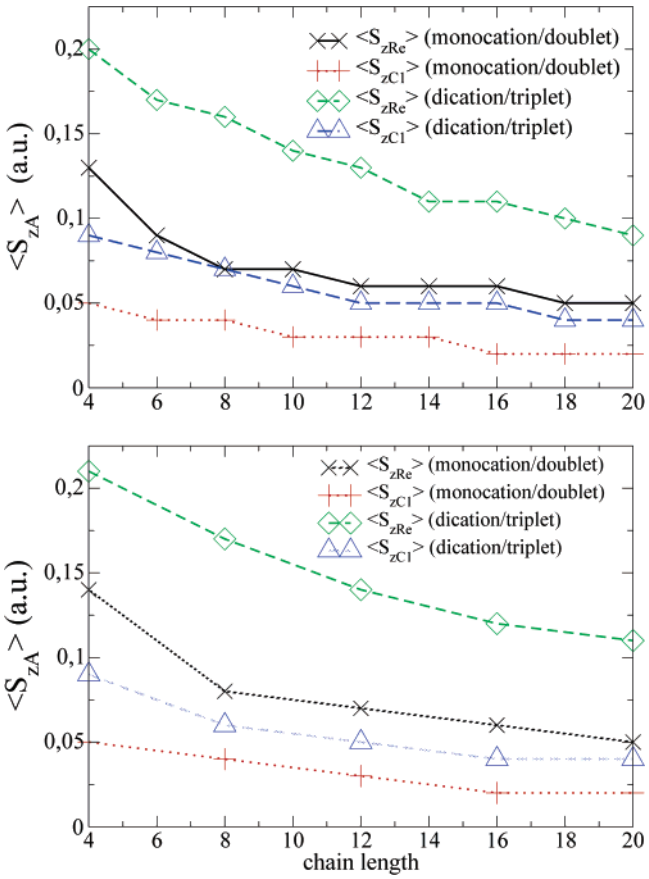

Figure 7. Local $\langle \hat{S}_z \rangle$ values for the rhenium atom and the carbon chain atom next to it for the monocation/doublet and the dication/triplet states. BP86/RI (top)/B3LYP* (bottom). The local $\langle \hat{S}_z \rangle$ values of all the individual carbon chain atoms do not differ by more than ±0.01 atomic units, so we have plotted only the values for the carbon chain atom which is next to the metal center.

atomic units) portion of electron spin. The differences between (○) and (•) become smaller as the distance from the metal atoms increases along the chain. This means that the electron spin is essentially located on selected atoms of the chain and not on the metal atom. For chain lengths of 8 carbon atoms and below, the spin distribution is asymmetric; that is, the spin is distributed according to the pattern (○)-(•)(○)(•)... which because of the even number of atoms in the chain starts with (•) on one rhenium atom and ends with (○) on the other one. This behavior shows that one metal center becomes subordinate to the other one and accepts this pattern. For longer chain lengths, the metal centers are so far apart that their influence on each other is weak enough to let each center have its own preferred pattern, thus leading to the symmetric spin distribution. Interestingly, the point where the spin distribution starts to become symmetric is, for both functionals, exactly the same point where the $HOMO_\alpha-LUMO_\alpha$ gap for the monocation/quartet state, displayed in Figure 6, is suddenly reduced. This indicates a change in the nature of the Slater determinant constructed from the Kohn−Sham orbitals that we are interpreting as an approximation of the wave function at this point. Of course, one may wonder how meaningful is the comparison of our data with a real physical phenomenon, as it may suffer from artifacts of the one-determinant approximation. However, our calculations indicate that in the case of the monocation/quartet state of the binuclear rhenium complex investigated here, a one-determinant description appears to be reasonable as soon as the carbon chain includes more than 8 atoms.

Here, our focus was on the question of whether the spin is located on the chain or on the metal atom. But when the local spin on the metal is high, some of this spin may be delocalized onto the other ligands, especially onto NO and, in some cases, onto the carbon atoms of the Cp* ligand, with local $\langle \hat{S}_z \rangle$ values up to 0.19 au in the case of the monocation/quartet state for a chainlength of 4 on the nitrogen atom near the metal center with $\langle \hat{S}_{zRe} \rangle = 0.39$. However, in most cases the local spin on the ligands is negligible, and the sum of local spins on rhenium and the chain atoms is approximately equal to the total $\langle \hat{S}_z \rangle$ expectation value.

In previous work, we have shown that although absolute local spin values can depend strongly on several parameters such as basis set, density functional, and in particular the local projector, the qualitative picture is much less affected by such dependencies.[46] A comparison of the BP86/RI and B3LYP* values in Figure 7 and Table 1 furthermore suggests that for the molecules analyzed here, the influence of the density functional on local $\langle \hat{S}_{zA} \rangle$ values is negligible. In addition, the spin contamination is very low in all cases (the total spin expectation value $\langle \hat{S}^2 \rangle$ is in the worst case equal

Table 1. Local Löwdin* $\langle \hat{S}_z \rangle$ Values for the Monocation/Quartet State for Several Chain Lengths[a]

chain length	$\langle \hat{S}_{zRe1} \rangle$	$\langle \hat{S}_{zC1} \rangle$	$\langle \hat{S}_{zC2} \rangle$	$\langle \hat{S}_{zC3} \rangle$	$\langle \hat{S}_{zC4} \rangle$	$\langle \hat{S}_{zC5} \rangle$	$\langle \hat{S}_{zC6} \rangle$	$\langle \hat{S}_{zC7} \rangle$	$\langle \hat{S}_{zC8} \rangle$	$\langle \hat{S}_{zC9} \rangle$	$\langle \hat{S}_{zC10} \rangle$	$\langle \hat{S}_{zRe2} \rangle$
4	0.09	0.16	0.03	0.18	0.02							0.39
6	0.08	0.14	0.02	0.15	0.00	0.17	0.01					0.34
8	0.08	0.13	0.02	0.14	0.00	0.15	0.00	0.15	0.02			0.27
10	0.08	0.15	0.05	0.13	0.07	0.10						
12	0.07	0.14	0.03	0.13	0.05	0.11	0.08					
14	0.06	0.13	0.03	0.13	0.03	0.11	0.05	0.08				
16	0.06	0.12	0.02	0.12	0.02	0.11	0.04	0.09	0.06			
18	0.05	0.11	0.02	0.11	0.02	0.11	0.03	0.09	0.05	0.07		
20	0.05	0.10	0.02	0.11	0.01	0.10	0.02	0.09	0.03	0.07	0.05	
4	0.08	0.17	0.01	0.19	0.00							0.41
8	0.06	0.14	0.00	0.15	−0.02	0.16	−0.02	0.16	0.00			0.30
12	0.05	0.16	0.02	0.14	0.04	0.12	0.07					
16	0.04	0.13	0.01	0.13	0.00	0.12	0.03	0.10	0.06			
20	0.03	0.12	0.00	0.13	0.00	0.12	0.00	0.11	0.02	0.08	0.05	

[a] Upper part: BP86/RI. Lower part: B3LYP*. For chains of 10 or more carbon atoms, the spin distribution is symmetric, so only the data for one rhenium atom and one side of the chain are given.

to 0.77, 3.83, and 2.09 for the monocation/doublet, monocation/quartet, and dication/triplet states, respectively, which does not differ much from the values for pure spin states, 0.75, 3.75, and 2.00). We recall that in order to interpret the local $\langle \hat{S}_{zA} \rangle$ values as a measure for local spin, the Slater determinants under study must not be spin-contaminated. Thus, the qualitative local $\langle \hat{S}_z \rangle$ distributions reported here may be regarded as a reliable representation of the electron spin distribution (but note that we interpret the Kohn−Sham determinant as a wave function here).

7. Conclusion

We have investigated spin-state splittings and the local electron spin distribution for the mono- and dications $\{[Re]-C_n-[Re]\}^{z+}$ with $[Re] = \eta^5$-$(C_5Me_5)Re(NO)(PPh_3)$ within a DFT framework (BP86/RI and B3LYP*) using Ahlrichs' TZVP basis set. The chain lengths range from $n = 4$ to 20.

One important result of this work is that the spin-state splittings from total energy expectation values may be estimated from the orbital energy splittings $HOMO_\beta-LUMO_\alpha$ in the low-spin state, which is always the ground state. Because the geometry optimization of the high-spin states is time-consuming for compounds of this size, this provides a valuable way to obtain a qualitative picture of the spin-state splittings at considerably reduced computational costs. In a similar spirit, the $HOMO_\alpha-LUMO_\alpha$ gaps, which decrease for increasing carbon chain lengths, have been interpreted as a qualitative measure for the energy difference to the first electronically excited state and for the ease of electron transport through the molecular wires.

Our calculations furthermore show an interesting behavior of the total spin-state splittings as the chain length increases from 4 to 20 carbon atoms: for both spin states, the splittings decrease with increasing chain length; while for the dications, no constant value of the singlet−triplet splitting is reached even at a chain length of 20, the doublet-quartet splitting reaches a constant value at long chain lengths of the monocations. Because this constant value is small with BP86/RI (10 kJ/mol) and even reduced when exact exchange is included (4 kJ/mol with B3LYP*), it might be possible that, for very long chain lengths, the high-spin state becomes the ground state.

The local spins reported in this work show that where the electron spin is mainly located in these molecules depends strongly on the total spin state. For the doublet state of the monocation and for the triplet state of the dication, the spin is located on the metal centers rather than on the chain, although there is some spin delocalization onto the chain. For chain lengths of 10 or more carbon atoms, the electron spin of the quartet state of the monocation is essentially located on the chain and not on the metal centers. For all of the systems under study, the individual local spins, as well as the spin polarization, decrease as the number of carbon atoms in the chain increase.

For future work, it would be interesting to extend these studies to sp carbon chains with other metal endgroups. Thus, one could determine if the spin splittings and local spins observed for $\{[Re]-C_n-[Re]\}^{z+}$ are a general feature of sp carbon chains with metal endgroups or if they depend on the nature of the metal. In addition, this would permit the determination of whether the spin-state splittings in such sp carbon chains can be generally estimated from the $HOMO_\beta-LUMO_\alpha$ splittings in the low-spin state.

Acknowledgment. This work was supported by the Deutsche Forschungsgemeinschaft DFG (Re 1703/A and collaborative research center SFB 583), and the Fonds der Chemischen Industrie (FCI). C.H. gratefully acknowledges funding by a Chemiefonds-Doktorandenstipendium of the FCI, and J.N. gratefully acknowledges funding by a Forschungsstipendium of the DFG. M.R. has been supported by a Dozentenstipendium from the FCI.

Supporting Information Available: Quantum chemical methodology and Cartesian coordinates for $[Re]-C_n-[Re]^{z+}$. This material is available free of charge via the Internet at http://pubs.acs.org.

IC050240L